

An experimental model of reflection and transmission of ocean waves by an ice floe

Alessandro TOFFOLI,¹ Alberto ALBERELLO,¹ Luke G. BENNETTS,²,
Michael H. MEYLAN,³ Claudio CAVALIERE,⁴ and Alexander V. BABANIN¹

¹*Centre for Ocean Engineering Science and Technology,
Swinburne University of Technology, Melbourne, VIC 3122, Australia*

E-mail: toffoli.alessandro@gmail.com

²*School of Mathematical Sciences, University of Adelaide, Adelaide, SA 5005, Australia*

³*School of Mathematical and Physical Sciences,
University of Newcastle, Callaghan NSW 2308, Australia*

⁴*Polytechnic University of Milan, Milan, 20133, Italy*

(Dated: December 3, 2024)

Abstract

An experimental model of reflection and transmission of ocean waves by an ice floe is presented. Evolution of mechanically-generated, regular waves is monitored in front and in the lee of a solitary, square floe, made of a synthetic material. Results confirm dependence of reflection and transmission on the period of the incident wave. Results also indicate that wave overwash on the floe affects reflection and transmission.

PACS numbers:

I. INTRODUCTION

Ocean surface waves penetrate tens to hundreds of kilometres into the sea ice-covered oceans. Wave motions force ice floes to bend and flex. This can cause the floes to fracture and, subsequently, to break into smaller floes. The region of ice-covered ocean that is broken by waves provides a convenient definition of the marginal ice zone for ice/ocean models, as the relatively small floes sizes are likely to affect the dynamic and thermodynamic properties of the ice cover [1, 2].

The waves themselves are affected by interactions with the floes. In particular, wave energy attenuates approximately exponentially with distance into the ice-covered ocean [e.g. 3]. There is also evidence that the directional wave spectrum becomes isotropic in the ice-covered ocean [4]. Wave scattering by floes can explain both exponential attenuation and spreading of the directional spectrum. However, comparisons between numerical scattering models and field data indicate that scattering cannot account for all of the attenuation experienced by waves [5, 6]. Dissipative processes, such as overwash (the wave running over the top of floes), floe-floe collisions, and viscoelasticity, must also be considered.

[7] and [1, 2] recently proposed a model of wave energy transport in the ice-covered ocean and concomitant wave-induced floe breaking. [8] and [9] proposed similar models of wave energy transport in the ice-covered ocean but without floe breaking over 15 years earlier. The wave energy transport models are based on a modified version of the energy balance equation [10], which includes a source term for wave-ice interactions, S_{ice} . The wave-ice term parametrizes directional scattering and dissipation of energy due to the presence of ice cover. The source terms that exist in the open ocean, i.e. wind input S_{in} and dissipation S_{ds} , is also modified in the ice-covered ocean, e.g. by scaling the terms according to the proportion of open ocean present [8, 11]. It is not yet clear how the nonlinear interaction term, S_{nl} , should be modified. The resulting balance equation reads as follows:

$$\frac{\partial E(f, \vartheta)}{\partial t} + \vec{C}_g \cdot \nabla E(f, \vartheta) = (1 - f_i)(S_{in} + S_{ds}) + S_{nl} + S_{ice}, \quad (1)$$

where $E(\tau, \vartheta)$ is the wave energy spectrum, as a function of frequency and direction (f and ϑ , respectively); \vec{C}_g is the group velocity; and f_i is the fraction of ice coverage.

In its most simple form, the wave-ice term is $S_{ice} = -f_i\alpha E/d$, where $f_i\alpha/d$ is the exponential attenuation rate of wave energy per metre due to ice cover. The quantity α is the

attenuation coefficient, and d is the average diameter of the floes. Using the model of [12], the attenuation rate is related to the proportion of incident wave energy transmitted by a single floe, Tr , via $\alpha = -\log(Tr)$. Note that, using this simple form for S_{ice} , all reflected wave energy is lost from the system. Alternatively, conservative, directional scattering can be incorporated, as outlined in [8], [9] and Meylan and Masson [13].

The attenuation rate is functionally dependent on wave period. Attenuation rates measured in field experiments range from approximately $8 \times 10^{-4} \text{ m}^{-1}$ for 8–9 s waves, to approximately $2 \times 10^{-4} \text{ m}^{-1}$ for long waves (periods > 10 s). Although, generally, attenuation rates increase with decreasing wave periods, a ‘roll-over’ effect, i.e. a decrease in attenuation for small wave periods (< 8 s) has been noted [4]. A summary of recorded attenuation rates is given in [14].

Field measurements are normally limited to mild wave conditions. Moreover, existing numerical attenuation models are linear. The functional dependence of the attenuation rate on wave height is, therefore, not properly understood yet. This includes the onset and subsequent contribution of highly non-linear processes, such as overwash.

In the present paper, we present an experimental model of wave reflection and transmission, and hence attenuation, by a floe. The experimental model was implemented in the coastal wave basin at the Coastal Ocean and Sediment Transport (COAST) laboratories of Plymouth University, UK. The floe is made of a synthetic elastic material, which bends and flexes with the wave motion. Regular waves of prescribed period and amplitude are generated mechanically. Wave elevation is measured by arrays of wave gauges before and after the floe. Despite the idealisations of the real-world phenomenon necessary in a laboratory setting, experimental facilities allow investigation of transmission in a controlled environment, in which the quantities of interest can be measured at high accuracy.

[15] and [16, 17] report experimental models of wave-floe interactions, which are closely related to the experimental model described here. However, the previous experiments employed an edge barrier to preclude overwash. We avoid use of the artificial edge barrier. Further, we provide evidence that overwash affects reflection and transmission properties of the floe, using measurements provided by a wave gauge located at the centre of the upper surface of the floe.

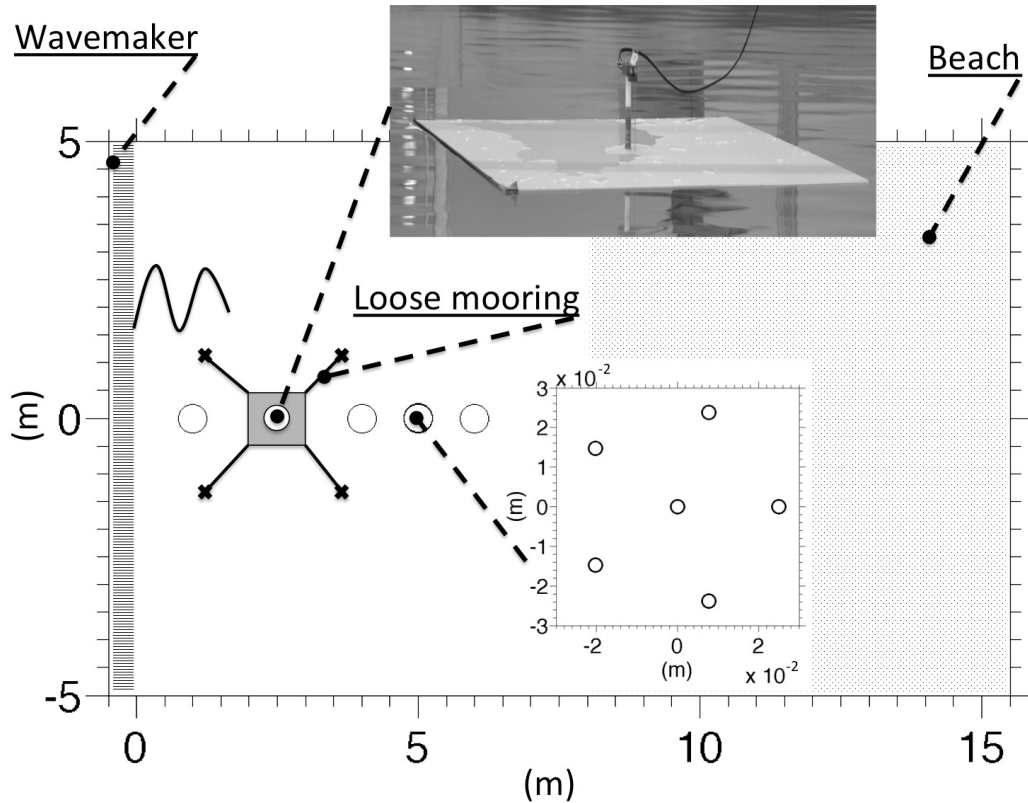


FIG. 1: Directional wave basin and experimental set-up.

II. LABORATORY EXPERIMENTS

The laboratory facility consists of a directional wave basin of width of 10 m, length 15.5 m and water depth 0.5 m (see Fig. 1). The tank is equipped with twenty individually controlled active-piston wave makers, which are capable of absorbing incoming waves by measuring the force on the front of the paddle and controlling the velocity [18]. At the opposite end, wave energy is dissipated by a beach of slope 1:10. A reflection analysis indicated that less than 1% of the wave energy is reflected backwards. Note that any residual waves reflected from the beach, off the surfaces of the model and from sides of the tank are absorbed by the active pistons.

At a distance of 2 m from the wave maker, a plastic sheet was deployed to simulate an ice floe. Two different types of plastic were tested: a polypropylene plastic with density of 0.905 g cm^{-3} and Young's modulus 1600 MPa; and PVC (FOREX®) plastic with density 0.500 g cm^{-3} and Young's modulus 500 MPa. Note that polypropylene has density similar to

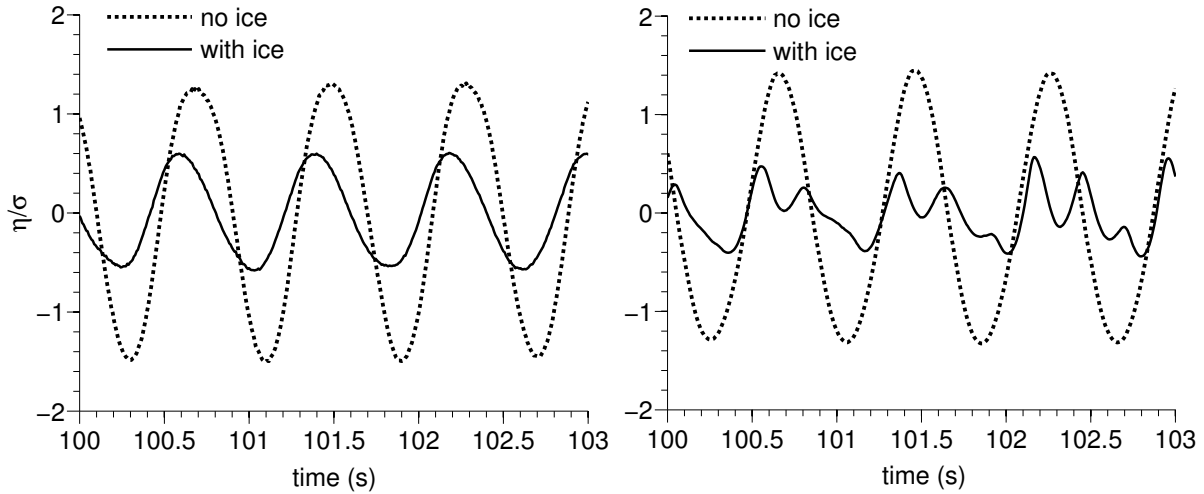


FIG. 2: Normalised surface elevation in the lee of a polypropylene plastic sheet of 5 mm for a wave field with period $T = 0.8$ s (wavelength 1 m) and steepness $ka = 0.15$.

sea ice but has different rigidity. PVC has a rigidity comparable to sea ice but substantially lower density, which results in a larger freeboard. Polypropylene sheets were provided with thicknesses 5 mm, 10 mm, 20 mm and 40 mm; PVC was provided with thicknesses 5 mm, 10 mm and 19 mm. The sheets were cut into square floes with side lengths $L_{plate} = 1$ m. The experimental set-up was designed to represent the full scale wave-ice interactions in scale 1:100.

A loose mooring was applied at the four corners of the floe to suppress drift, whilst maintaining the six rigid-body degrees of freedom (heave, surge, sway, pitch roll and yaw) and elastic motions. At the wave maker, waves were generated by imposing three different wave periods, namely $T = 0.6$ s, 0.8 s, and 1 s, with corresponding wavelengths $L_{wave} = 0.56$ m, 1 m and 1.56 m, respectively. The wave fields therefore tested conditions in which the waves were shorter than, equal to and longer than the floe. The wave amplitude, a , was selected so that the wave steepness ka , where k is the wavenumber, matched the following values: 0.04 , 0.08 , 0.1 and 0.15 . This range includes gently sloping waves ($ka = 0.04$ and 0.08) as well as storm-like waves ($ka = 0.1$ and 0.15), without reaching the breaking limit.

The water surface elevation, η , was monitored with capacitance gauges at a sampling frequency of 128 Hz. One gauge was deployed approximately 1 m in front of the floe to

capture the incident and reflected waves. In the lee of the floe, three probes were deployed every metre to track the evolution of the transmitted wave field. At 2 m from the rear edge of the floe a six-probe array, arranged as a pentagon of radius of 0.25 m and a middle probe, was deployed to monitor the directional properties of the wave field. In order to quantify the depth of overwash (and concurrent wave motion), a mini-gauge was deployed in the middle of the upper surface of the floe (see photo in Fig. 1). Its weight was a negligible small fraction of the floe's weight. For each configuration, five-minute time series were recorded.

III. RESULTS

A. Reflection and transmission

Fig. 2 shows an example of time series provided by a wave gauge in the lee of the floe for gently sloping waves ($ka = 0.04$, left panel) and storm-like waves ($ka = 0.15$, right panel). The corresponding time series from a control test, conducted without the floe, is also shown. The transmitted waves for the gently sloping incident waves retain a regular profile. In comparison, the transmitted waves for the storm-like incident waves are erratic, i.e. irregular. The origin of the erratic behaviour is not clear. Influence of the mooring system cannot be ruled out. However, we attribute the behaviour to floe impacts on the water surface.

Due to the erratic behaviour of the transmitted waves for storm-like incident waves, we quantify reflection and transmission in terms of significant wave heights, which is defined as 4σ , where σ is the standard deviation of the recorded time series. Let the significant wave height of the incident wave, from the control tests, be denoted H_i ; the significant wave height in front of the floe is denoted H_{front} ; and in the lee of the floe is denoted H_{rear} . Reflection and transmission coefficients are computed as $R = (H_{front}/H_i) - 1$ and $T = H_{rear}/H_i$, respectively. Note that the estimation of an average wave height based on a rigorous zero-crossing analysis leads to an identical value of the reflection and transmission coefficients.

Average reflection and transmission coefficients, as functions of a normalised wavelength (i.e. a ratio of wavelength to floe length), for the different wave steepness and plate thickness are presented in Figs. 3 and 4 (polypropylene and PVC, respectively). Significant variation

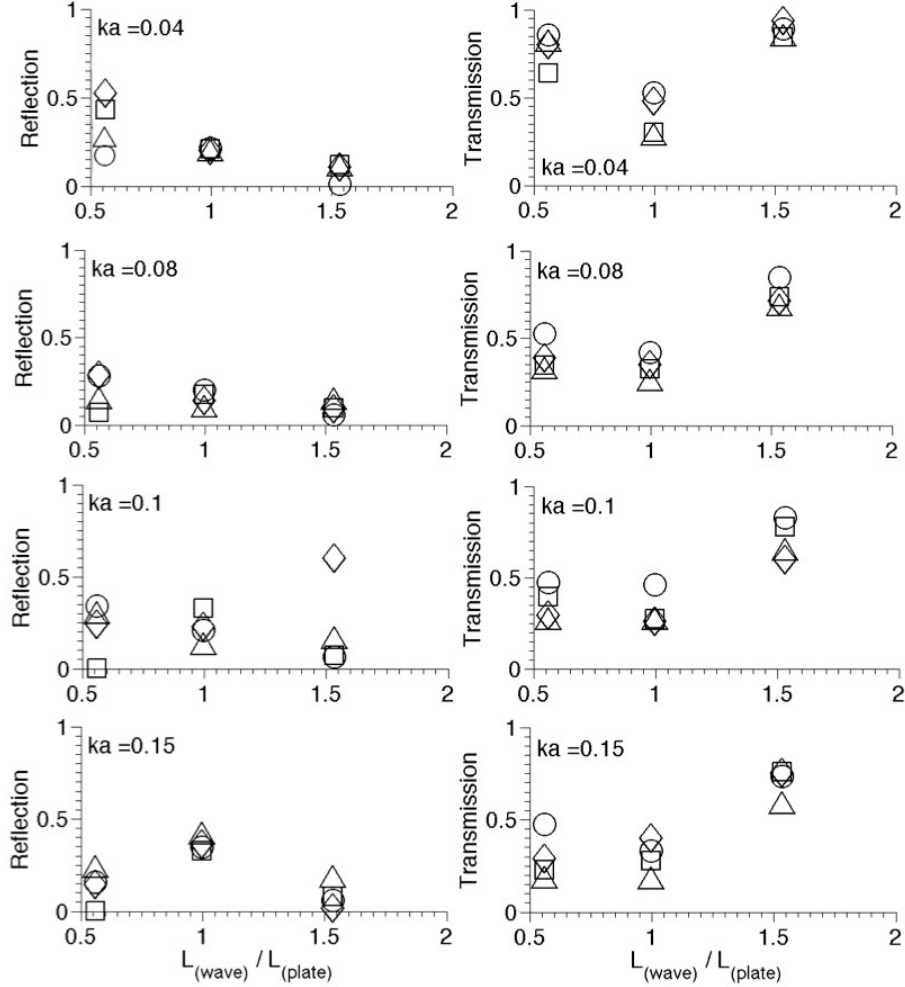


FIG. 3: Average transmission coefficient (T) against the normalised wavelength as a result of the interaction with a polypropylene floe: thickness = 5mm (o); thickness = 10 mm (Δ); thickness = 20 mm (\square); and thickness = 40 mm (\diamond).

of reflection and transmission with wavelength, thickness and steepness are evident.

At the front edge of the plate, a portion of the incident wave is back-scattered. For low wave steepnesses, reflection increases with increasing floe thickness, in agreement with predictions of linear models [e.g. 19]. However, the relationship between reflection and thickness becomes more complicated for larger steepnesses.

Decreasing reflection as wavelength increases is also apparent for low steepness waves. This is also consistent with numerical models [e.g. 20]. The relationship becomes more complicated for larger steepnesses although it is approximately maintained for all steepnesses by the more compliant PVC floes.

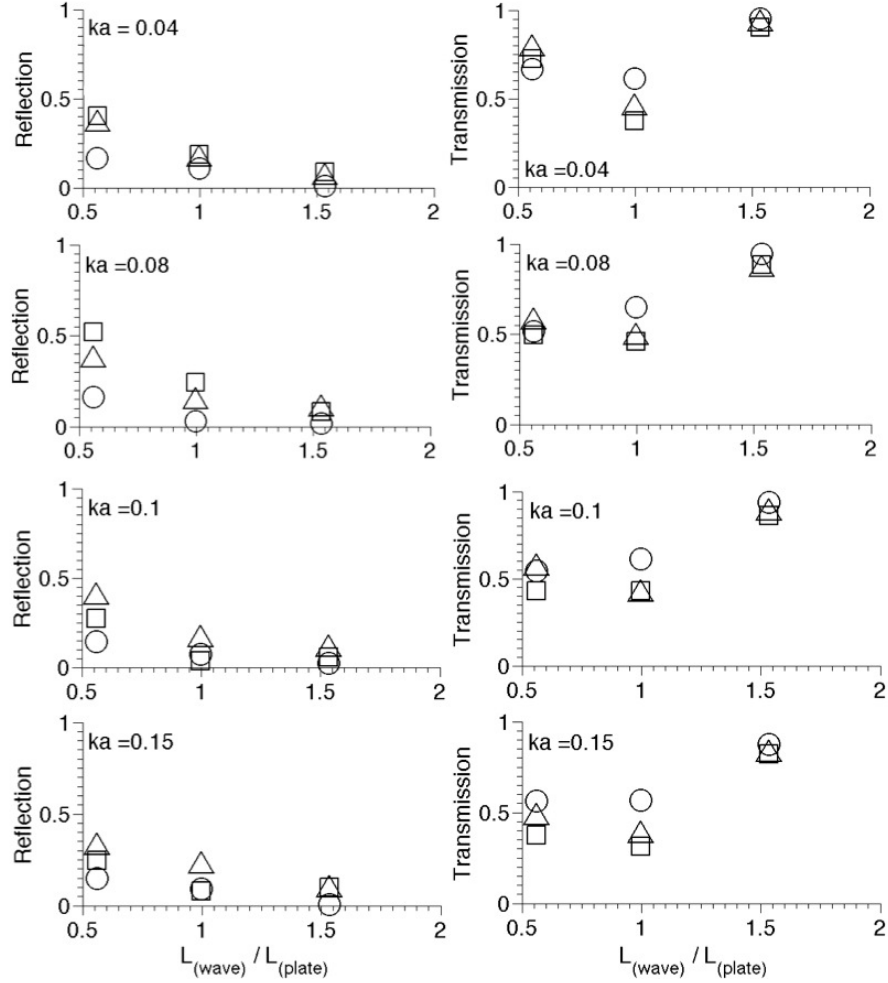


FIG. 4: Average transmission coefficient (T) against the normalised wavelength as a result of the interaction with a PVC floe: thickness = 5 mm (o); thickness = 10 mm (Δ); thickness = 19 mm (\square).

It would be reasonable to expect that, for low wave steepnesses, the transmission coefficient would follow a complementary monotonic increasing trend with increasing wavelength. However, the experimental data do not show this expected behaviour. Instead, transmission is minimum for a wavelength equal to the floe length. This resembles the rollover in attenuation found in field data, although we do not claim that our findings are responsible for the rollover phenomenon.

As waves become more energetic (that is to say, wave steepness increases), wave reflection generally reduces. The difference is most pronounced for shorter waves. Strikingly, reductions in reflection for larger steepnesses are matched by reductions in transmission. The

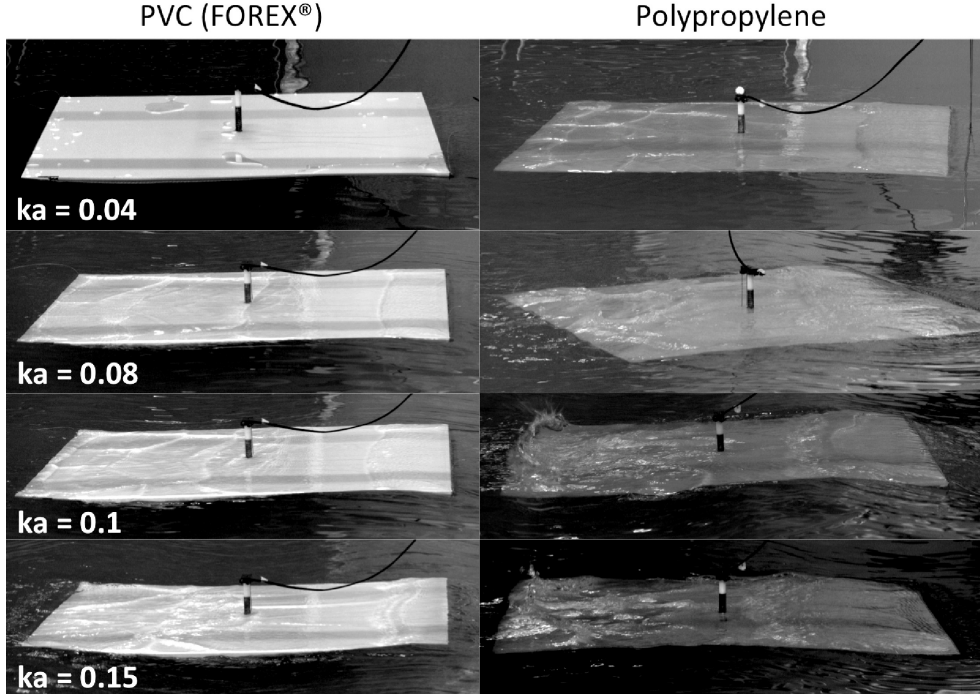


FIG. 5: Overwash of a polypropylene floe (right panels) and PVC floe (left panels) for a wave field with wavelength equal to the plate length and plate thickness of 10 mm.

decrease in transmission is also most significant for shorter waves. This results in a qualitative change in the dependence of transmission on wavelength, so that the ‘rollover’ effect is diminished. For $ka \geq 0.08$, transmission is approximately constant for $L_{wave}/L_{plate} \leq 1$, and then increases for the longest wave (see bottom panels in Figs. 3 and 4). Despite some scatter, transmission trends are the same for the polypropylene and PVC floes. The more compliant PVC floes do, however, transmit a larger proportion of the waves.

We note that preliminary tests did not show any significant effects of mooring on the transmitted wave field. Nonetheless, owing to the complexity and intensity of wave-induced ice motion (especially in the most severe wave conditions), we cannot exclude that the observed wave fields might have been affected somehow by the applied mooring.

B. Effect of overwash

Low steepness waves gently propagate through the floe and hence attenuation is attributed to wave reflection and any energy lost during the flexure of the floe. However, the propagation of energetic waves is far more complicated. In particular, waves overwash the

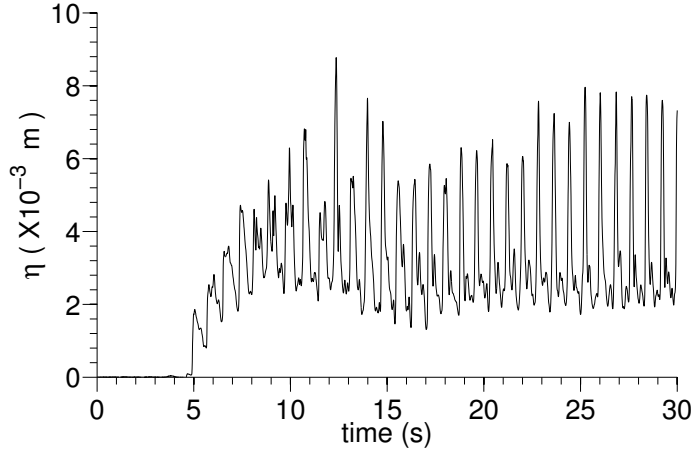


FIG. 6: Example of water surface elevation over a polypropylene plastic sheet of thickness 10mm in a wave field of wavelength 1m and steepness $ka = 0.15$.

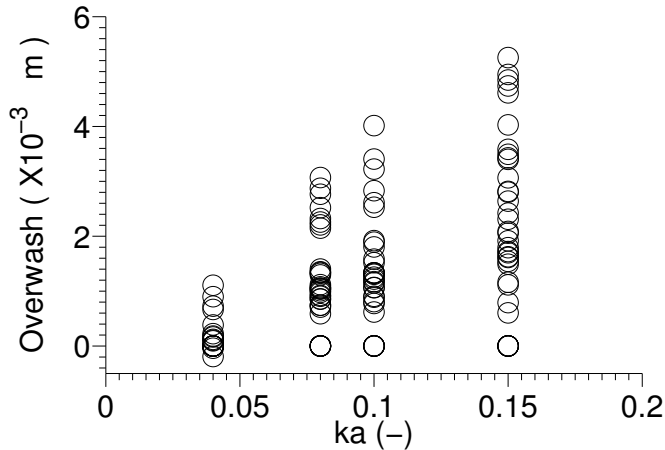


FIG. 7: Overwash depth as a function of wave steepness.

floe. As a consequence, the floe is submerged by the wave, either partially or fully. Further, shallow water waves propagate in the overwashed fluid. These waves are generated at both ends of the floe and interact with each other. Therefore, wave fields may substantially steepen in the overwashed region. This often results in wave breaking and hence energy dissipation, thus contributing to attenuation. Examples of the overwash behaviours described above are shown in Fig. 5 for different wave steepnesses.

With the occurrence of overwash, part of the wave energy propagates directly over the floe, and, thus, is no longer reflected by the front edge of the sheet. This helps to explain the slight

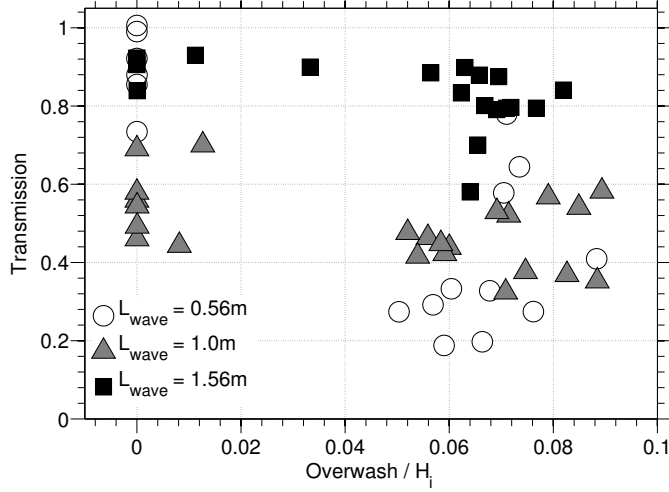


FIG. 8: Transmission as a function of normalised overwash depth for polypropylene floes.

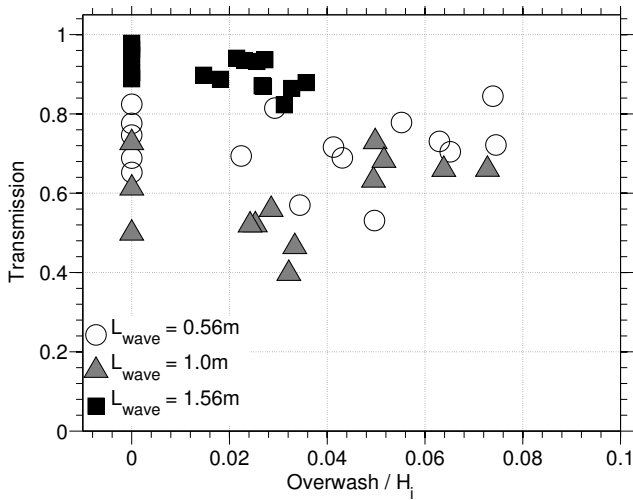


FIG. 9: As in Fig. 8 but for PVC floes.

reduction in the reflection coefficient observed for more energetic wave fields. Dissipation of wave energy in the overwashed fluid helps explain the reduction of transmission observed for more energetic waves.

The depth of overwashed fluid and, hence, wave motion over the floe was measured by a wave gauge. Fig. 6 shows an example time series provided by the wave gauge. From here on, overwash depth refers to the time series mean. Dependence of overwash depth on steepness is confirmed in Fig. 7.

The relationship between transmission and overwash depth is shown in Figs. 8 and 9,

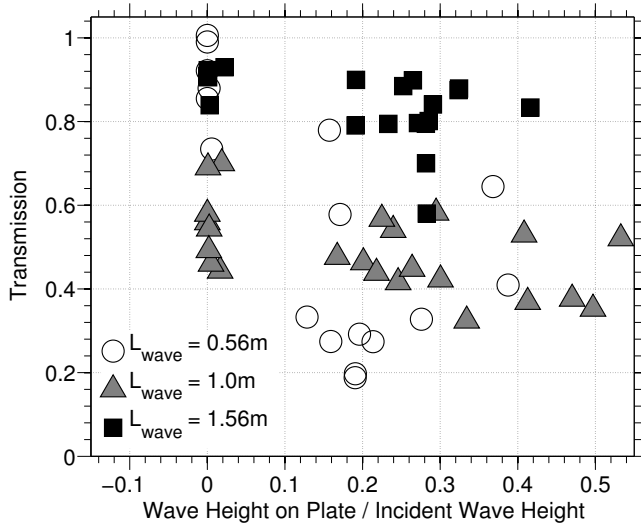


FIG. 10: Transmission as a function of normalised overshoot significant wave height for polypropylene floes.

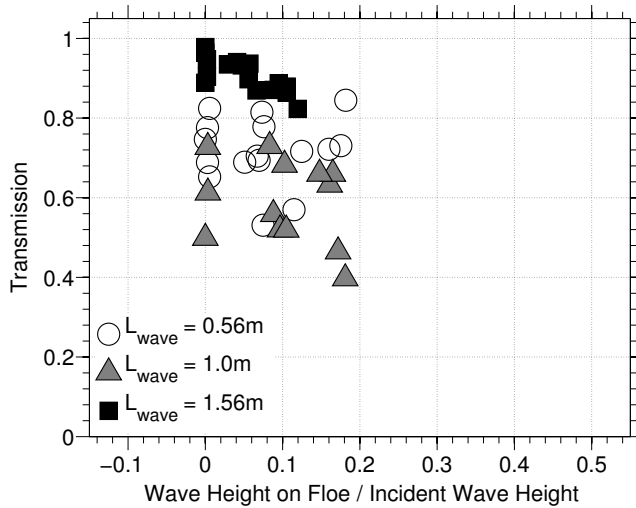


FIG. 11: As in Fig. 10 but for PVC floes.

for the polypropylene and PVC floes, respectively. Overshoot depth is normalised by the incident wave height. It is evident that the mechanical properties of the floe affect overshoot depth. In particular, overshoot depth is larger for the polypropylene floes, which have smaller freeboards than the PVC floes.

An overall trend of reducing transmission with increasing overshoot depth is evident. The relationship is most clear for the polypropylene floes. Monotonic reduction of transmission

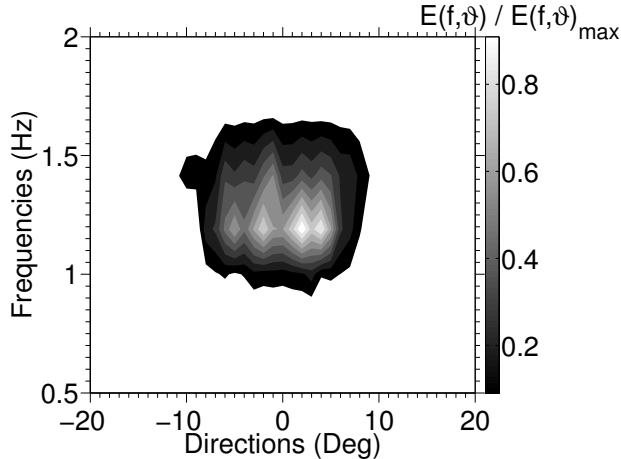


FIG. 12: Wave directional spectra in the lee of the floe for $L_{wave}/L_{plate} = 1$ and $ka = 0.15$.

only occurs for the longest waves ($L_{wave} = 1.56$ m). For shorter waves, there is normally a sudden drop of the transmission when normalised overwash depth exceeds approximately 0.02. Transmission then further decreases with increasing overwash depth, albeit at a very small rate for polypropylene floes. In comparison, for the PVC floes there is some evidence of overturning, leading to increasing transmission, for deeper overwash. Note that, eventually, transmission seems to level off for the largest overwash depths.

The correlation between transmission and normalised overwash depth is weak. Overwash depth only estimates a uniform layer of water over the plate and it does not consider the intensity of wave activity. We therefore consider transmission as a function of the significant wave height of the overwashed fluid (normalised with respect to the incident wave height) in Figs. 10 and 11. The relationship between transmission and overwash significant wave height follows a more consistent trend. In particular, there is a monotonic decrease of transmission with increasing significant wave height. The rate of decrease is, largely, insensitive to wavelength, although data are more scattered for shorter waves.

C. Directional scattering

The directional scattering of the transmitted wave field is here estimated from the full directional spectrum $E(f, \vartheta)$ as measured by the six-probe array. Reconstruction of the directional distribution of wave energy is performed using a wavelet directional method [21].

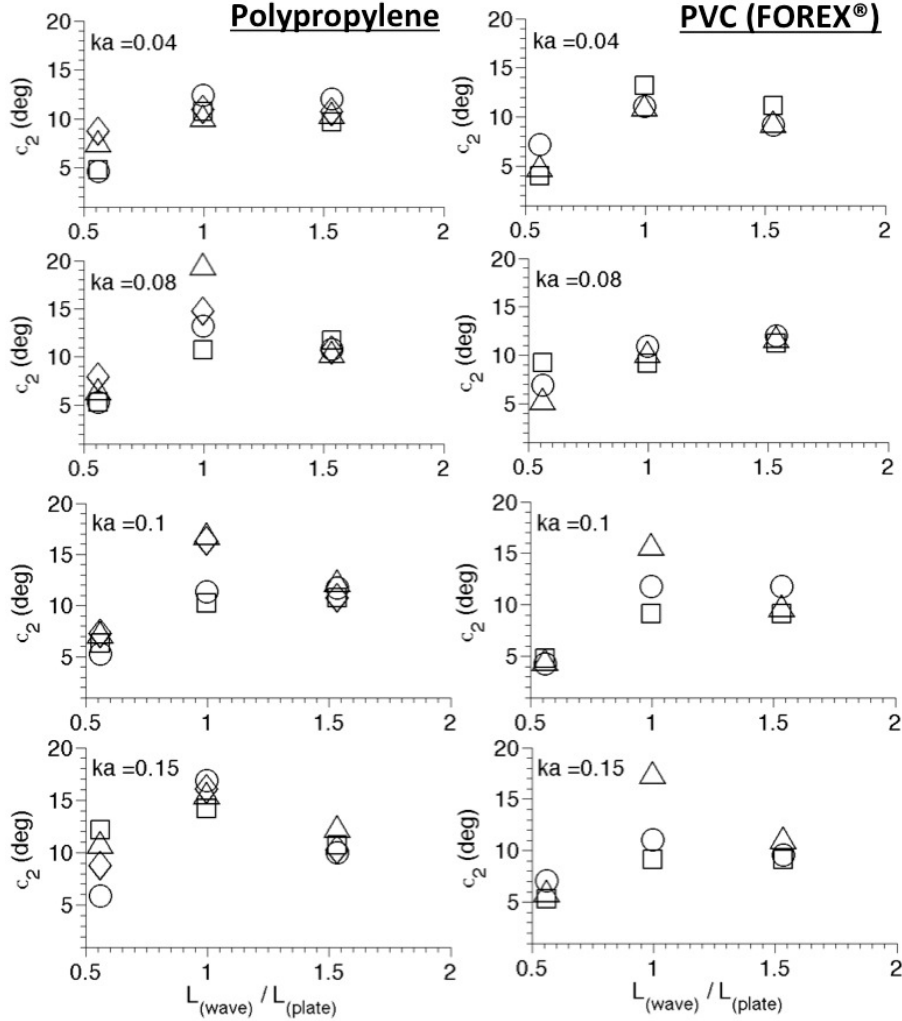


FIG. 13: Directional spreading in the lee of the plate as a function of the normalised wavelength. Polypropylene in left panels: thickness = 5 mm (o); thickness = 10 mm (Δ); thickness = 20 mm (\square); and thickness = 40 mm (\diamond). PVC (FOREX®) in right panels: thickness = 5 mm (o); thickness = 10 mm (Δ); thickness = 19 mm (\square).

Fig. 12 shows an example of a recorded spectrum. Note that the scattered wave field does not consist of one dominant wave component with directional spreading, i.e. a unimodal sea. Instead, it appears to be composed of a few dominant components with a narrow directional spreading (four in the example of Fig. 12), propagating along slightly different directions (multimodal sea state) and with comparable frequencies. A measure of the directional spread is extracted by performing the following integration:

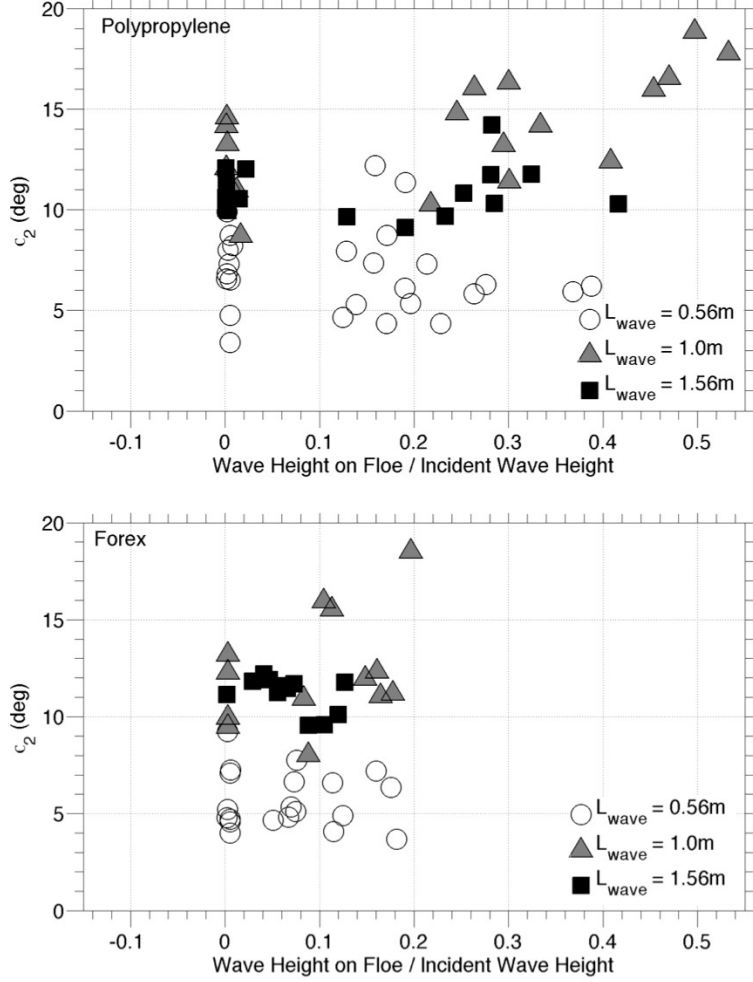


FIG. 14: Directional spreading as a function of the normalised wave height on the plate.

$$\sigma_2(f) = \left(\frac{\int_0^{\pi/2} \vartheta^2 E(f, \vartheta) d\vartheta}{\int_0^{\pi/2} E(f, \vartheta) d\vartheta} \right)^{1/2}, \quad (2)$$

[cf. 22, 23] where f is the frequency of the incident wave.

Fig. 13 shows the directional spread as a function of wavelength normalised with respect to the floe length. The magnitude of the spreading is smallest for the smallest wavelength. Further, the magnitude of spreading is approximately equal for wavelengths equal to the floe length and approximately 1.5 times the floe length. Changes in wave steepness, floe thickness and mechanical properties of the floe do not affect the directional scattering notably.

Fig. 14 shows the directional spread as a function of normalised overwash significant

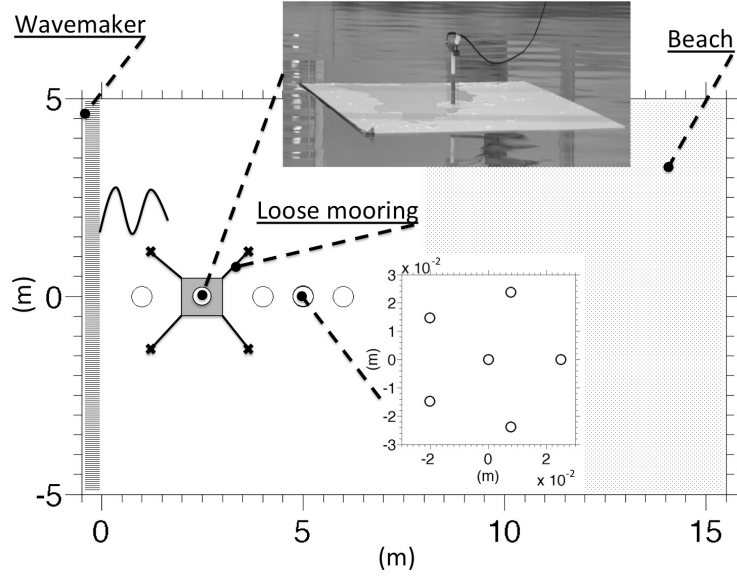


FIG. 15: Transmission as a function of directional spreading.

wave height. For the shortest waves ($L_{wave} = 0.56$ m), the directional scatter does not vary significantly with the overwash wave height. However, for wavelengths equal to and longer than the floe length (i.e. $L_{wave} = 1.0$ m and 1.56 m), an apparent broadening of the wave spectrum takes place for increasing overwash wave height. This is particularly evident for the less compliant polypropylene, as it is subjected to a broader range of overwash.

Fig. 15 shows transmission as a function of the directional spreading, in order to verify dependence of wave attenuation on directional scattering. The cloud of data indicates large scatter, especially for shorter waves. On the whole, there is no indication here that transmission is affected by the directional spreading for the shortest and longest wavelengths. Conversely, there is a clear trend for decreasing transmission with increasing directional spreading when the wavelength and floe length are equal.

IV. CONCLUSIONS

An experimental model of reflection and transmission of ocean waves by a solitary ice floe has been reported. The experimental tests were conducted in the coastal directional wave basin of Plymouth University, using regular incident waves with different wave periods, amplitudes and steepnesses. Wave fields were selected to range from mild to storm-like conditions. The floe was modelled by a square plastic sheet. Two different plastics were

used, and different thicknesses were tested. The wave elevation in front of the floe and in its lee was measured by an array of wave gauges. Only the overall amount of wave energy was analysed to estimate reflection and transmission coefficients. Wave overwash of the floe was measured by a mini wave gauge that was deployed in the centre of the upper surface of the floe.

The following key conclusions were drawn from the data:

1. Wave reflection in the experiments is qualitatively consistent with linear numerical model for low wave steepnesses, i.e. reflection increases for thicker floes, and decreases for longer waves. However, these relationships are not maintained for large steepnesses.
2. Transmission cannot be inferred from reflection. Even for the most gentle wave steepness, the transmission is not monotonic with wavelength, instead taking a minimum when the wavelength is equal to the floe length.
3. In general, overwash increases as wave steepness increases. Transmission decreases slightly with increased depth of the overwashed fluid (normalised with respect to the incident wave height), and more significantly with the significant wave height of the waves in the overwashed fluid.
4. The floes produce notable directional scattering. Transmitted wave energy is generally distributed over a few dominant directions. No evidence was found to indicate that directional scattering affects wave transmission for the longest and shortest wavelengths tested. However, there is evidence that transmission is affected by directional spreading for waves with length equal to the floe length, with transmission decreasing as directional spreading increases.

V. ACKNOWLEDGEMENTS

Experiments were supported by the Small Research Grant Scheme of the School of Marine Science and Engineering of Plymouth University and performed when AT and AA were appointed at Plymouth University. LB acknowledges funding support from the Australian Research Council (DE130101571) and the Australian Antarctic Science Grant Pro-

gram (Project 4123).

- [1] T. D. Williams, L. G. Bennetts, D. Dumont, V. A. Squire, and L. Bertino, *Ocean Mod.* **71**, 81 (2013).
- [2] T. D. Williams, L. G. Bennetts, D. Dumont, V. A. Squire, and L. Bertino, *Ocean Mod.* **71**, 92 (2013).
- [3] V. A. Squire and S. C. Moore, *Nature* **283**, 365 (1980).
- [4] P. Wadhams, V. A. Squire, D. J. Goodman, A. M. Cowan, and S. C. Moore, *J. Geophys. Res.* **93**, 6799 (1988).
- [5] A. L. Kohout and M. H. Meylan, *J. Geophys. Res.* **113** (2008).
- [6] L. G. Bennetts, M. A. Peter, V. A. Squire, and M. H. Meylan, *J. Geophys. Res.* **115** (2010).
- [7] D. Dumont, A. L. Kohout, and L. Bertino, *J. Geophys. Res.* **116**, doi:10.1029/2010JC006682 (2011).
- [8] D. Masson and P. LeBlond, *J. Fluid Mech.* **202**, 111 (1989).
- [9] M. H. Meylan, V. A. Squire, and C. Fox, *J. Geophys. Res.* **102**, 22981 (1997).
- [10] G. Komen, L. Cavaleri, M. Donelan, K. Hasselmann, H. Hasselmann, and P. Janssen, *Dynamics and modeling of ocean waves* (Cambridge University Press, Cambridge, 1994).
- [11] W. Perrie and Y. Hue, *J. Phys. Oceanogr.* **26**, 1705 (1996).
- [12] L. G. Bennetts and V. A. Squire, *Proc. R. Soc. Lond. A* **468**, 136 (2012).
- [13] M. H. Meylan and D. Masson, *Ocean Modelling* **11**, 417 (2006).
- [14] J. Schulz-Stellenfleth and S. Lehner, *J. Geophys. Res.* **107**, 20 (2002).
- [15] A. L. Kohout, M. H. Meylan, S. Sakai, K. Hanai, P. Leman, and D. Brossard, *Journal of Fluids and Structures* **23**, 649 (2007).
- [16] F. Montiel, F. Bonnefoy, P. Ferrant, L. G. Bennetts, V. A. Squire, and P. Marsault, *J. Fluid Mech.* **723**, 604 (2013).
- [17] F. Montiel, L. G. Bennetts, V. A. Squire, F. Bonnefoy, and P. Ferrant, *J. Fluid Mech.* **723**, 629 (2013).
- [18] S. H. Salter, in *Directional Wave Spectra Applications* (ASCE, 1981), pp. 185–202.
- [19] M. H. Meylan and V. A. Squire, *J. Geophys. Res.* **99**, 891 (1994).
- [20] I. V. Lavrenov and A. V. Novakov, Tech. Rep. Transport and fate of contaminants in the

northern seas. Sea ice project package. AARI final report (2000), URL http://transeff.npolar.no/transport/Ice/aari_all.pdf.

- [21] M. A. Donelan, W. M. Drennan, and A. K. Magnusson, *J. Phys. Oceanogr.* **26**, 1901 (1996).
- [22] P. A. Hwang, W. D. W., E. J. Walsh, W. B. Krabill, and R. N. Swift, *J. Phys. Oceanogr.* **30**, 2768 (2000).
- [23] A. Toffoli, M. Onorato, E. M. Bitner-Gregersen, and J. Monbaliu, *J. Geophys. Res.* **115**, C03006 (2010).